

Finite element modeling of machining nickel superalloy produced by direct energy deposition process

Careri, Francesco; Imbrogno, Stano; Attallah, Moataz M.; Essa, Khamis; Umbrello, Domenico

DOI:

[10.1016/j.promfg.2020.04.120](https://doi.org/10.1016/j.promfg.2020.04.120)

License:

Creative Commons: Attribution-NonCommercial-NoDerivs (CC BY-NC-ND)

Document Version

Publisher's PDF, also known as Version of record

Citation for published version (Harvard):

Careri, F, Imbrogno, S, Attallah, MM, Essa, K & Umbrello, D 2020, 'Finite element modeling of machining nickel superalloy produced by direct energy deposition process', *Procedia Manufacturing*, vol. 47, pp. 525-529.
<https://doi.org/10.1016/j.promfg.2020.04.120>

[Link to publication on Research at Birmingham portal](#)

General rights

Unless a licence is specified above, all rights (including copyright and moral rights) in this document are retained by the authors and/or the copyright holders. The express permission of the copyright holder must be obtained for any use of this material other than for purposes permitted by law.

- Users may freely distribute the URL that is used to identify this publication.
- Users may download and/or print one copy of the publication from the University of Birmingham research portal for the purpose of private study or non-commercial research.
- User may use extracts from the document in line with the concept of 'fair dealing' under the Copyright, Designs and Patents Act 1988 (?)
- Users may not further distribute the material nor use it for the purposes of commercial gain.

Where a licence is displayed above, please note the terms and conditions of the licence govern your use of this document.

When citing, please reference the published version.

Take down policy

While the University of Birmingham exercises care and attention in making items available there are rare occasions when an item has been uploaded in error or has been deemed to be commercially or otherwise sensitive.

If you believe that this is the case for this document, please contact UBIRA@lists.bham.ac.uk providing details and we will remove access to the work immediately and investigate.

23rd International Conference on Material Forming (ESAFORM 2020)

Finite Element Modeling of Machining Nickel Superalloy Produced By Direct Energy Deposition Process

Francesco Careri^{a,b}, Stano Imbrogno^b, Moataz M. Attallah^b, Khamis Essa^c, Domenico Umbrello^{a,*}^a*Department of Mechanical, Energy and Management Engineering, University of Calabria, Via P. Bucci Cubo 46c, 87036 Rende, Italy*^b*School of Metallurgy and Materials, University of Birmingham, Edgbaston, Birmingham B15 2TT, United Kingdom*^c*School of Mechanical Engineering, University of Birmingham, Edgbaston, Birmingham B15 2TT, United Kingdom** Corresponding author. Tel.: +44-(0)121-414-7899 ; E-mail address: s.imbrogno@bham.ac.uk

Abstract

Direct Energy Deposition (DLD) is a generative manufacturing method for metals and it is usually employed to build near-net-shape components starting from powder, through a layer-by-layer production strategy. This process provides an opportunity to fabricate complex shaped and functionally parts mainly used in high performance engineering areas, such as aerospace and automotive industry. However, the metal parts produced frequently do not satisfy the tolerances as well as the surface quality, therefore the post-process finishing operations as machining are normally considered as a valid solution to satisfy the geometrical requirements. During the design phase, the finite element simulation results a fundamental tool to help the engineers in the correct decision of the most suitable process parameters, especially in manufacturing processes, in order to produce products of high quality. The aim of this work is to develop a 3D finite element model of turning operation of Nickel Superalloy Inconel 718, produced via Direct Energy Deposition (DLD). A customized user sub-routine was built-up in order to model the mechanical behavior under machining operations of as deposited condition to predict the main fundamental variables as cutting forces and temperature.

© 2020 The Authors. Published by Elsevier Ltd.

This is an open access article under the CC BY-NC-ND license (<https://creativecommons.org/licenses/by-nc-nd/4.0/>)

Peer-review under responsibility of the scientific committee of the 23rd International Conference on Material Forming.

Keywords: Finite Element Model; Machining; Additive Manufacturing; Nickel Superalloy

1. Introduction

The Additive Manufacturing (AM) technologies offer a new method, faster and more flexible, to manufacture complicated parts. AM allows to generate a component through a layer-by-layer building strategy, avoiding the significant amount of material waste that characterize the traditional subtractive manufacturing processes. In the past decade, the various AM technologies have received considerable attentions and are reaching a predominant role in all the industrial sectors. [1].

The Direct Laser Deposition (DLD) is an AM technique that allows to create or repair components through layer-by-layer deposition of material that is melted via high-powered laser. Nowadays, DLD potentially represents an innovative manufacturing technique in aerospace, medical or military industries because of its high flexibility [1, 2]. Compared to

other AM process (e.g. Selective Laser Melting), the DLD is also suited for large parts with coarse features that require high deposition rates.

The *Inconel 718* is an age-hardenable nickel-base superalloy which is characterized by a γ matrix reinforced by precipitation strengthening phases known as γ' and γ'' . This alloy is employed in applications characterized by extreme operative conditions because of its good strength and excellent resistance to oxidation at high operating temperatures. For this reason, the *Inconel 718* is considered one of the key materials used in aircraft engine components. In this context, the DLD manufacturing techniques shown its benefits in performing repair or producing the *Inconel 718* complex components with a relatively lower cost than the conventional manufacturing techniques. The advantage of the AM techniques in relation to this material is mainly justified by the reason that the *Inconel*

718 is also known as a difficult-to-cut material. Indeed, during the machining process, the cutting forces and the temperatures developed within the interface between the tool and the workpiece drastically reduce the tool life increasing the production costs. However, the components produced or repaired by DLD generally require post-processing operations (e.g. finish machining) in order to achieve the surface quality and geometrical tolerances required from most of the practical applications. [3]. Therefore, the study of the machinability of the additively manufactured parts allows to optimize the cutting parameters in order to minimize or avoid the phenomena that reduce the tool life affecting thus the surface quality. [4-6]. Within this context, another significant role is represented by the numerical simulation, that allows a significant reduction of the experimental costs in the industrial process. In literature, most of the constitutive models that describe the mechanical behavior of the *Inconel 718* are mainly related to the wrought conditions (e.g. after heat treatment applications) where the material shows an equiaxial microstructure that is not realistically representative of the one produced by AM. Recently, Yuan et al. developed a material constitutive model for the *Inconel 718* characterized by a columnar dendritic microstructure and that exhibits an anisotropy in texture due to the DLD production process [7]. However, no applications of this model in machining simulations are available in literature since most of the manuscripts take into account the wrought material, consequently simpler constitutive model (e.g. Johnson-Cook) are considered and are not able to describe the thermo-mechanical behavior of the materials produced by AM [7].

Therefore, the aim of this work is to develop a Finite Element Model (FEM) of machining using the anisotropy constitutive material model that accurately describes the mechanical behavior of the *Inconel 718* produced by DLD process. The empirical equation reported in [7] was implemented via user-routine in order to predict the forces and temperatures during the machining process. The FEM was validated by comparing the numerical and experimental results.

2. Experimental and numerical procedure

2.1. Experimental procedure

The samples manufactured via DLD were cylindrical bars (120mm length and 33mm of diameter) made of *Inconel 718* Nickel superalloy. The chemical composition of the powder base material (wt.%) was: 54.45Ni, 18.18Cr, 18.19Fe, 4.88Nb, 2.9Mo, 0.91Ti, 0.42Al, 0.03Si, 0.02Ta, 0.01C, 0.002S, 0.01N, 0.011O. The samples were produced with a Trumpf TLC 1005 (5axis cnc machine) equipped with a TruDisk 4002 disk laser. The process parameters set were a laser power of 400W, 275mm/min of scan speed and 9.8g/min of powder flow rate. The scan strategy adopted to realize the bars is shown in Fig. 1a, the deposition was continuous and rotated of 90° layer by layer, the layer thickness kept constant to a value of 0.5mm, and longitudinal direction of the bar is aligned with the Z build direction. As expected, the microstructure was characterized by columnar dendritic grains that growth epitaxially from the substrate and are mainly oriented along the Z build direction

<100>.

The deposited material is characterized by elongated coarse grains crossing several deposit layers and normally shows a dendritic microstructure, with element segregations within the dendrites. Laves phase, rich in Nb, Mo, and Ti, in the interdendritic regions and carbide, typical Ti and Nb segregation. [8-9].

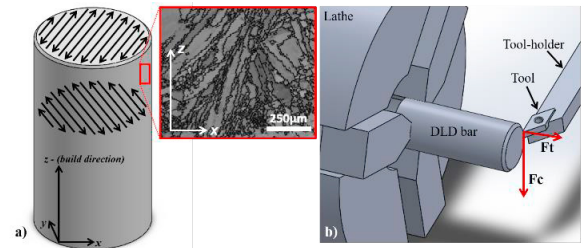


Fig. 1. (a) DLD bars and scan strategy schematization; (b) Machining test set up schematization.

The bars were machined after the deposition process on a CNC MAZAK high speed CNC turning center under dry condition. Regarding tool and tool holder employed during the tests, the Sandvik Coromant® DNMG 15 06 12-SMR S05F and Sandvik Coromant® DDJNR 2525M 15 were used respectively.

During the machining tests, schematized in Fig. 1b, three level of cutting speed (70, 90 and 120m/min) and two level of feed rate (0.1 and 0.2mm/rev) were selected. The depth of cut was kept constant and equal to 0.5mm due to the high surface roughness obtained through the DLD deposition process. During the turning test, the main cutting and thrust force were acquired by a KISTLER type 9257 B three components piezoelectric dynamometer while the temperature into the cutting zone was evaluated through an IR camera (Flir A6000). The material emissivity necessary for the accurate temperature measurement (being the temperature proportional to the emitted radiation) was calibrated comparing the measurements carried out with the infrared camera and with a thermocouple while a sample was warmed on a plate at fixed steps of temperature. The emissivity value computed was equal to 0.5. Subsequently, some samples were collected by the machined bars to evaluate the effects of the different cutting parameters in terms of the affected layer (plastically deformed material) beneath the machined surface through electron microscopy (SEM).

2.2. Material behaviour constitutive model

The most representative material behaviour model reported in literature related to the *Inconel 718* with a columnar dendritic microstructure is the one proposed by Yuan et al. [7]. Indeed, they considered the state of the material as produced by DLD without any further heat treatment, therefore very similar to the one considered in this work. The choice of this model instead of the well-known Johnson-Cook is mainly related to the anisotropy effect incorporated into the model. Indeed, it is well known that the microstructure of the parts produced by DLD manifests a preferential growth direction leading to unavoidable anisotropic behaviour of the material [7,10-12].

The constitutive material behaviour model is reported in Equation 1.

$$\sigma = \bar{\sigma}_G(T, \varepsilon) + \bar{\sigma}_a + \bar{\sigma}^*(\varepsilon, T, \dot{\varepsilon}) \quad (1)$$

where $\bar{\sigma}_G$ is the equivalent anisotropy component, $\bar{\sigma}_a$ the athermal component and $\bar{\sigma}^*$ the equivalent thermally activated component. T , ε and $\dot{\varepsilon}$ represent the temperature, the equivalent plastic strain and strain rate respectively. According with [7] the equivalent anisotropy component was obtained analysing the initial grain structure of the as deposited material. For further detail related to the constitutive model, the reader can consult the [7] since the limited space to represent the entire mathematical approach of the material behaviour model.

The as deposited *Inconel 718* grains had an orientation along the Z build direction (columnar dendrites) as expected by the DLD process. The geometry of the single grain was simplified into an ellipsoid as showed in Fig.1(a) according to [7]. The average major axis $2\hat{a}=687\mu\text{m}$ and minor axis $2\hat{b}=166\mu\text{m}$ were calculated as reported in Fig. 2.

In order to assume the mechanical anisotropy, the force that the grain is undergone due to the tool action was evaluated through the point M. This point is characterized by a polar angle $\theta=35^\circ$ and it was evaluated considering the two cutting forces that existed because of the interaction between the tool and the workpiece during the turning process, represented in Fig. 2.

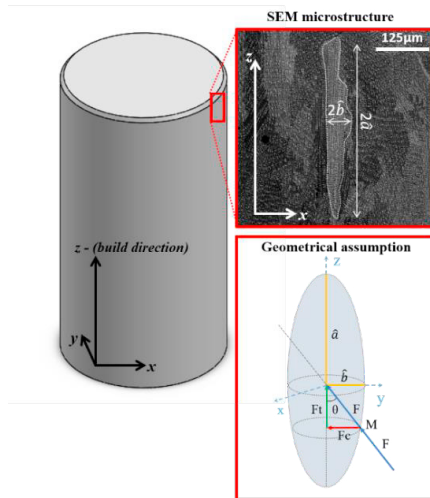


Fig. 2. Geometrical assumption of the columnar dendritic grain shape considered into the material behaviour model.

The Young's Modulus at room temperature used for the as deposited material $E=154\text{GPa}$ was found in literature [13] taking into account the material with the same microstructural and hardness characteristics.

2.3. FE model

The empirical models were implemented into the FE software via user sub-routines in order to predict the cutting forces and temperatures depending on the material and cutting conditions. The 3D FE model of the turning operation was developed on a commercial FE code SFTC DEFORM 3D. The

cutting tool was assumed as a rigid body while the workpiece was considered as a plastic body. It is important to highlight that some geometrical aspects such as the cutting edge ($20\mu\text{m}$) of the tool were considered in order to improve the predictive capability of the FE model. The tool and the workpiece were meshed with 50000 and 110000 tetrahedral elements respectively. Moreover, around the tool nose and on the workpiece machined surface the mesh was refined (average element size of $5\mu\text{m}$). A dynamic local remeshing window (remeshing zone), showed in Fig. 3b, was set following the tool motion. The kinematic and boundary conditions were set as showed in Fig.3a according to the experimental tests performed. In particular, the bottom and side surface of the workpiece were fixed in x, y, z directions, while the tool was allowed to move.

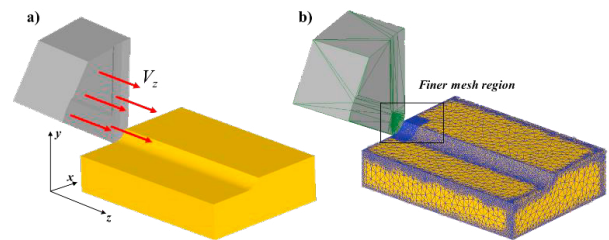


Fig. 3. a) kinematic and boundary condition; b) Refined mesh region.

It is worth to highlight that during the modelling of the workpiece, due to the anisotropic behaviour of the material, the columnar dendrites were oriented along the build direction that was parallel to the longitudinal axis of the bars. Into the FE domain, this direction was oriented to z direction. Concerning the thermal boundary conditions, on the bottom and side faces of the workpiece the temperature was set equal to the room temperature, as well as the back part of the tool. The top surface of the workpiece was able to exchange heat with the environment, as well as the top face of the tool as showed by Fig. 4.

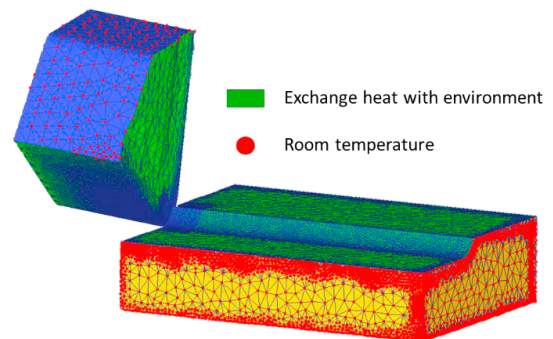


Fig. 4. Thermal boundary condition of the FE Model.

The interval time step was set equal to $2.5 \cdot 10^{-6}\text{s}$. To take into account the phenomena that occur into the contact region between the tool and the chip a hybrid sticking-sliding friction model (m and μ coefficients) was employed. The heat transfer at the tool-chip interface was set equal to $100,000\text{ kW/m}^2\text{K}$.

[14]. Setting this high value the thermal steady-state at the tool-chip-workpiece interfaces was reached within a short simulation time (10^{-3} – 10^{-4} s) by means of the assumption of thermally perfect contact under high cutting pressures. Moreover, a calibration procedure (trial and error) was carried out in order to define the friction coefficients value. In particular, two cutting conditions $V_c=70\text{m/min}$, $f=0.1\text{mm/rev}$ and $V_c=120\text{m/min}$, $f=0.2\text{mm/rev}$, were considered in the calibration procedure and the friction coefficient determined were equal to $\mu=0.05$ and $m=0.2$. The calibration procedures were ended when the average error representative of the average error of the cutting forces and temperatures was lower than 10%. Finally, the validation procedure was carried out to verify the reliability of the FE developed model in predicting the cutting forces and temperature.

3. Results and discussion

In Fig. 5 the comparison between the experimental and numerical cutting forces are reported. In general, both the cutting forces numerically predicted show the same experimental trends. In particular, The predicted main cutting forces is always slightly overestimated and the highest error (17%) was observed when 70m/min and 90m/min with a feed rate of 0.1mm/rev are used, while considering all the other case studies the error was lower than 8% (Fig. 5a). Concerning the feed forces showed in Fig. 5b, the predicted ones resulted lower than the experimental ones although they perfectly showed the same trend. This problem is due to different issues: the number of elements used into the cutting zone might led to a lower accuracy in predicting the forces since more elements usually allow to better approximate the round shape of the cutting edge. This results in an improved contact between the nodes of the mesh and the tool tip surfaces, therefore the missing contact between the tool and the workpiece (due to the bodies penetration) that usually cause the cutting force decrease is seriously reduced. On the other hand, increasing the number of elements into the cutting zone can drastically increase the computational time, therefore this further mesh optimization procedure was neglected since the main cutting forces were already predicted with a very low error and they are mainly related to power consumption that is usually more interesting from the manufacturing process view point. Another reason can be related to the anisotropic behavior showed by the as-deposited material due to the columnar dendritic grains. Indeed, the material behaviour model considers the grains oriented along the z build direction while in the reality a small amount resulted oriented randomly affecting the cutting forces.

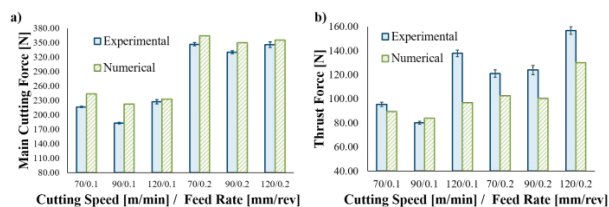


Fig. 5. Experimental and numerical results comparison of the (a) main cutting forces and (b) thrust forces.

Finally, since the tool geometry unavoidably changes, due to the wear effect. This aspect was not modelled because of higher computational time, therefore, the higher error in feed forces was also attributed to the absence of tool wear that introduces significant non-linearity in the friction and contact modeling, which are unavoidably present in the machining of superalloys [15]. Concerning the temperature, the numerical results were collected taking into account the frontal part of the chip as done with the experimental results from the frames acquired by the IR camera. The final result was obtained considering the average value of all the steps analysed after simulation reached the steady state condition. The results are reported in Fig. 6 and the trend showed by the simulated temperature is following the one obtained by the experiments.

Although, the *Inconel 718* is known as a difficult-to-cut material, the one produced by DLD process showed an unexpected ductility. Indeed, during the turning test, the formation of the chip was almost continuous varying the cutting forces and the feed rate. A frame acquired by the IR camera shows the continuous chip formation during the test performed with a cutting speed of 120m/min and feed rate of 0.2mm/rev (Fig. 6). It is important to highlight that the model can simulate the continuous chip formation but not its segmentation as occurred during the experimental tests (Fig. 6). The highest error of the predicted temperature was represented by the test with the cutting speed of 90m/min and feed rate of 0.1mm/rev and it was equal to 7.5%.

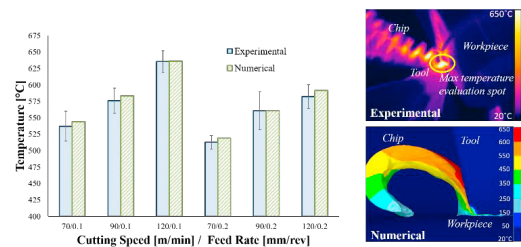


Fig. 6. Comparison of the experimental and numerical temperature (Numerical and IR camera frame $V_c=120\text{m/min}$, $f=0.2\text{mm/rev}$)

Fig. 7 represents the comparison between the affected layer observed by SEM and the one predicted by the FE model. In detail, the effective plastic strain was plotted on the cross section of the machined workpiece. Usually the numerical evaluation of the plastic strain of the material plastically deformed beneath the machined surface helps to understand if the metallurgical alterations (e.g. dynamic recrystallization) and hardening or recovery of the material (e.g. increase or decrease of the hardness) were occurring.

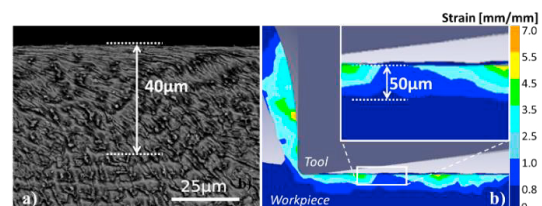


Fig. 7. Experimental (a) and numerical (b) results of machined affected layer of test ($V_c=120\text{m/min}$, $f=0.2\text{mm/re}$).

In Fig. 7a it is possible to observe that the machining process mainly affected a region of approximately $40\mu\text{m}$ where the grains resulted bended toward the cutting direction and extremely deformed near the machined surface. In Fig.7b is reported the affected layer predicted by the FE model taking into account the plastic strain calculated into the steady state part of the simulation. In this case the affected layer is approximately $50\mu\text{m}$ and it refers to plastic strain into the workpiece and the average level of deformation into the measured layer is equal to 3mm/mm .

The difference between the numerical and the experimental affected layer could be caused by the size of internal elements used to build the mesh. Indeed, during the simulation the remeshing occurs due to the sever deformation of the elements and some elements with different sizes are used by the software to rebuild the mesh undeformed. The size of these elements can slightly be higher the grain size observed in Fig. 7a, therefore the plastic deformation resulted slightly overestimated into the machined part.

4. Conclusion

In this paper, a new FE model able to predict the machinability (in terms of cutting forces and temperatures) of the as-deposited DLD *Inconel 718* is presented. One of the innovative aspects is the anisotropic behavior of the additively manufactured material included into the material behavior model that allowed to predict the behavior of the material during the machining process. Indeed, depending on the orientation of the grains, the two geometrical parameters $2\hat{a}$, $2\hat{b}$ and the angle θ allowed to adapt the model to the observed microstructure during the machining process. The FE model was validate comparing the numerical with the experimental cutting forces and temperatures. Furthermore, a qualitative prediction of the affected layer caused by the machining operation is reported and a comparison with an experimental result is showed.

References

- [1] Thompson SM, Bian L, Shamsaei N, Yadollahi A. An overview of direct laser deposition for additive manufacturing; Part I: Transport phenomena, modeling, and diagnostics. *Addit Manuf* 2015;8:36-62.
- [2] Shamsaei N, Yadollahi A, Bian L, Thompson SM. An overview of direct laser deposition for additive manufacturing; Part II: Mechanical behavior, process parameter optimization and control. *Addit Manuf* 2015;8:12-35.
- [3] Dutta B, Froes FS. The additive manufacturing (AM) of titanium alloys. *Met Powder Rep* 2017;72(2):96-106.
- [4] M'Saoubi R, Axinte D, Soo SL, Nobel C, Attia H, Kappmeyer G, Engin S, Sim WM. High performance cutting of advanced aerospace alloys and composite materials. *CIRP Ann Manuf Technol* 2015;64(2):557-580.
- [5] Pervaiz S, Rashid A, Deiab I, Nicolescu M. Influence of Tool Materials on Machinability of Titanium and Nickel-Based Alloys: A Review. *Materials and Manufacturing Processes* 2014;29:219-252.
- [6] Sharman ARC, Hughes JJ, Ridgway K. Workpiece surface integrity and tool life issues when turning Inconel 718 nickel based superalloy. *Machining Science and Technology* 2004;8(3):399-414.
- [7] Yuan K, Guo W, Li P, Zhang Y, Li X, Lin X. Thermomechanical behavior of laser metal deposited Inconel 718 superalloy over a wide range of temperature and strain rate: Testing and constitutive modeling. *Mechanics of Materials* 2019;135:13-25.
- [8] Parimi LL, Clark RGAD, Attallah MM. Microstructural and texture development in direct laser fabricated IN718. *Mater Charact* 2014;89:102–111.
- [9] Ding RG, Huang ZW, Li HY, Mitchell I, Baxter G, Bowen P. Electron microscopy study of direct laser deposited IN718. *Mater Charact* 2015;106:324-337.
- [10] Yuan K, Guo W, Li P, Wang J, Su Y, Lin W, Li Y. Influence of process parameters and heat treatments on the microstructures and dynamic mechanical behaviors of Inconel 718 superalloy manufactured by laser metal deposition. *Mater Sci Eng* 2018A;721:215-225.
- [11] Zhong C, Gasser A, Kittel J, Wissenbach K. Improvement of material performance of Inconel 718 formed by high deposition-rate laser metal deposition. *Mater Des* 2016;98:128-134.
- [12] Zhang DY, Niu W, Cao XY, Liu Z. Effect of standard heat treatment on the microstructure and mechanical properties of selective laser melting manufactured Inconel 718 superalloy. *Mater Sci Eng A* 2015;644:32-40.
- [13] Baufeld B. Mechanical Properties of INCONEL 718 Parts Manufactured by Shaped Metal Deposition (SMD). *JMEP* 2012;21(7):1416–1421.
- [14] Arrazola PJ, O'zel T, Umbrello D, Davies M, Jawahir IS. Recent Advances in Modelling of Metal Machining Processes. *CIRP Annals* 2013;62(2):695–718.
- [15] Melkote SN, Liu R, Zelaia PF, Marusich T. A physically based constitutive model for simulation of segmented chip formation in orthogonal cutting of commercially pure titanium. *CIRP Ann Manuf Technol* 2015;64:65-68